

## Proteomic and physiological responses in mangrove *Kandelia candel* roots under short-term high-salinity stress

Jianhong XING<sup>1,2</sup>, Dezhuo PAN<sup>1</sup>, Lingxia WANG<sup>3</sup>, Fanglin TAN<sup>4</sup>, Wei CHEN<sup>1,\*</sup>

<sup>1</sup>College of Life Sciences, Fujian Agriculture and Forestry University, Fuzhou, Fujian, China

<sup>2</sup>College of Resources and Chemical Engineering, Sanming University, Sanming, Fujian, China

<sup>3</sup>College of Life Sciences, Ningxia University, Yinchuan, Ningxia, China

<sup>4</sup>Fujian Academy of Forestry Sciences, Fuzhou, Fujian, China

Received: 13.06.2019 • Accepted/Published Online: 20.09.2019 • Final Version: 14.10.2019

**Abstract:** *Kandelia candel* is one of the mangrove species that are most resistant to environmental stress. As a typical nonsalt-secreting mangrove plant, *K. candel* is an ideal biological material to analyze the molecular mechanism of salt tolerance in woody plants. In this study, changes in protein abundance and expression profile in *K. candel* roots under high-salinity stress of 600 mmol L<sup>-1</sup> NaCl were analyzed using isobaric tags for relative and absolute quantification (iTRAQ) assay. Moreover, the physiological parameters associated with metabolic pathways in which the differentially abundant proteins (DAPs) are involved were determined. A total of 5577 proteins were identified by iTRAQ analysis of the *K. candel* root proteins, of which 227 were DAPs with a fold change ratio >1.2 or a fold change ratio <0.83 and a P-value <0.05. A total of 227 DAPs consisting of 110 up-regulated and 117 down-regulated proteins were identified. Our Gene Ontology (GO) and Kyoto Encyclopedia of Genes and Genomes (KEGG) pathway analyses revealed that the DAPs were primarily involved in biological processes including carbohydrate and energy metabolisms, stress response and defense, cell wall structure, and secondary metabolism. The results of the physiological parameters showed that their profile changes were consistent with those of the proteome analysis. The results of the proteome and physiological parameters showed that *K. candel* roots could resist high-salinity stress by maintaining a normal Embden-Meyerhof-Parnas and tricarboxylic acid (EMP-TCA) pathway, increasing the activities of various antioxidant enzymes and antioxidant contents, stabilizing the cell wall structure, and accumulating secondary metabolites such as triterpenoids.

**Key words:** Proteome, energy metabolism, cell wall, antioxidation, triterpenoids

### 1. Introduction

Salt stress is one of the primary abiotic stresses that affect plant growth and global crop yields (Miyazaki et al., 2007; Song et al., 2011). A high-salinity environment can cause ionic toxicity, osmotic stress, and oxidative damage to plant cells, affect photosynthetic biological processes, respiration, and energy metabolism, and eventually leads to plant growth arrest or even death. Simultaneously, soil salinization causes a decline in land productivity and seriously threatens the sustainable development of agriculture and forestry (Bandehagh et al., 2011; Kosová et al., 2011). Therefore, it is very important to study the salt tolerance mechanisms of plants, excavate salt tolerance genes, and cultivate new salt-tolerant varieties.

Proteomics technology provides an effective method for studying plant adaptation to abiotic stresses; thus, it has been widely used to understand the molecular mechanisms of plant salt stress (Tuteja, 2007; Soni et al., 2015). Isobaric

tags for relative and absolute quantification (iTRAQ) technology developed in recent years can efficiently and accurately detect the changes of protein content, providing an effective technical platform for detailed analysis of molecular mechanisms of plant salt stress responses (Gong et al., 2014; Cheng et al., 2016). Proteomic changes in model plants, major crops and some halophytes under salt stress have previously been analyzed by iTRAQ technique in *Arabidopsis thaliana* and *Thellungiella halophila* (Pang et al., 2010), *Gossypium hirsutum* L. (Li et al., 2015; Gong et al., 2017), *Oryza sativa* L. (Xu et al., 2015a), *Glycine max* cv Dongnong 50 (Ji et al., 2016), maize inbred lines Jing724 and D9H (Luo et al. 2017), *Triticum aestivum* (Jiang et al., 2017), *Musa paradisiaca* (Ji et al., 2019), and *Halogeton glomeratus* (Wang et al., 2016a). These studies demonstrated that photosynthesis, carbohydrate and energy metabolism, signal transduction, membrane transporters, stress responses, and defense all

\* Correspondence: weichen909@163.com

played important roles in response to salt stress in roots and leaves.

Proteome studies on salt tolerance mechanisms of mangrove plants have also been reported. Zhu et al. (2012) analyzed the proteomic changes of *Bruguiera gymnorhiza* roots under salt stress using 2-DE technique and found that fructose-1,6-diphosphate aldolase (FBP) protein is up-regulated in the primary roots, while an osmotic regulatory protein in the lateral roots was up-regulated at early stages of stress. Therefore, the trend of protein expression was inconsistent with that of the corresponding gene expression. A 2-DE study of proteins in *Avicennia marina* leaves under salt stress showed that nitric oxide (NO) signaling pathway improves salt tolerance by enhancing photosynthesis, energy and primary metabolisms (Shen et al., 2018b). In our previous studies, we investigated the changes in chloroplast proteins in *K. candel* seedling leaves in response to salt stress using iTRAQ technique. It has been proven that photosynthesis, respiration and energy metabolism, signal transduction, osmotic regulation, Na<sup>+</sup> compartmentalization, and antioxidant metabolism play important roles in salt tolerance of *K. candel* species (Wang et al., 2014, 2015, 2016b).

The mangrove *K. candel* is a type of woody halophyte that grows in the intertidal zones of tropical and subtropical oceans. During a long evolutionary process, *K. candel* formed a unique salt tolerance mechanism which enables it to withstand up to 600 mmol L<sup>-1</sup> salt stress (Wang et al., 2014). Therefore, it is an ideal system to analyze the salt tolerance mechanism of woody plants. The root is the first organ injured by salt stress in plants. Therefore, it is important to investigate the proteomic changes of the *K. candel* root under salt stress to reveal its molecular strategies in relation to salt tolerance. In this study, iTRAQ quantitative proteomics was used to analyze protein abundance and expression patterns in *K. candel* seedling roots under high-salinity stress. Enhanced carbohydrate and energy metabolism, antioxidative activity, cell wall structure stability, and metabolism of secondary metabolites in *K. candel* roots were found under salt stress in this study. The findings improve our understanding of the mechanisms of salt tolerance in the woody halophyte.

## 2. Materials and methods

### 2.1. Plant materials and salt treatment

The hypocotyls of *K. candel* were collected from the Zhangjiangkou Mangrove Nature Reserve, Zhangzhou City, Fujian Province (23°55' N, 117°26' E). Hypocotyls of similar size and maturity that are free of any form of physical damage, including damages due to pests or disease manifestation, were planted in plastic pots of 45 × 35 × 25 cm. Hoagland nutrient solution was added to the sand culture. The lost water was supplemented every evening, and the nutrient solution was replaced every three days

(Wang et al., 2016b). Until the plant grew four leaves (60 days), the seedlings were irrigated with Hoagland nutrient solution without NaCl (control group) and 600 mmol L<sup>-1</sup> NaCl. The roots of the seedlings were collected 72 h after treatment, and the roots were wrapped in aluminum foil and frozen in liquid nitrogen for 10 min, and then stored at -80 °C for future use. Three biological repeats were performed for each treatment.

### 2.2. Total protein extraction and iTRAQ labeling

Total protein was extracted using a phenol method described by Wang et al. (2014). Approximately 2 g of *K. candel* root was rapidly ground into fine powder in liquid nitrogen, and 10 mL of phenol extraction buffer (0.1 mol L<sup>-1</sup> Tris, 0.05 mol L<sup>-1</sup> ascorbic acid (AsA), 0.1 mol L<sup>-1</sup> KCl, 0.05 mol L<sup>-1</sup> disodium tetraborate decahydrate, 1% (v/v) Triton X-100, and 2% (v/v) β-mercaptoethanol) were added to the mixture and mixed well. An equal volume of Tris-saturated phenol (pH 8.0) was added and vortexed for 10 min. After centrifugation at 5500 × g for 10 min at 4 °C, the phenol layer was transferred to a new tube and mixed with a 6-fold volume of precooled 0.1 mol L<sup>-1</sup> ammonium acetate methanol solution and precipitated overnight at -20 °C. After centrifugation at 20,000 × g for 20 min at 4 °C, the precipitate was suspended in 10 mL of precooled methanol for 1 h at -20 °C. After centrifugation at 20,000 × g for 20 min at 4 °C, the precipitate was suspended in 10 mL of precooled acetone with 0.07% β-mercaptoethanol for 1 h at -20 °C. After centrifugation at 20,000 × g for 20 min at 4 °C, the step above was performed once more, and the protein powder was stored at -80 °C.

Next, 0.5 mol L<sup>-1</sup> tetraethylammonium bicarbonate (TEAB) was added and the protein powder was sonicated at 200 W for 20 min, centrifuged at 25,000 × g for 20 min at 4 °C, and the supernatant was absorbed. The protein concentration was determined using the Bradford method (Bradford 1976). Typically, 100 μg of protein from each group was added to 5 μg of trypsin and incubated at 37 °C for 12 h. The lysed peptides were then stored in 0.5 mol L<sup>-1</sup> TEAB. Following the manufacturer's instructions for the iTRAQ Reagent-8 Plex Multiplex Kit (Applied Biosystems, Foster City, CA, USA), the samples were labeled with tags 114, 115, and 116 for the 600 mmol L<sup>-1</sup>NaCl group and tags 117, 118, and 119 for the control group. Each group contained three biological repeats.

### 2.3. SCX classification and LC-ESI-MS/MS analysis

The labeled peptide solutions were mixed and loaded onto a PolySULFOETHYL 4.6 × 100 mm column (5 μm, 200 Å, PolyLC Inc., Maryland, USA) for gradient elution, followed by desalination with a C18 Cartridge (66872-U, Sigma, Phenomenex, Torrance, CA, USA) and freeze-dried (Unwin et al. 2010).

Peptide solution samples were separated using a nano-high performance liquid chromatography (HPLC) system Easy nLC (Thermo Fisher Scientific, San Jose, CA, USA).

The samples were loaded onto a Thermo Scientific EASY column (2 cm × 100 μm, 5 μm-C18), eluted and separated using a Thermo Scientific EASY column (75 μm × 100 mm, 3 μm-C18) at a flow rate of 300 nL min<sup>-1</sup>. The elution settings were as follows: 0% to 50% B solution (0.1% (v/v) formic acid and 84% (v/v) acetonitrile) for 55 min; 50% to 100% B solution for 2 min; 100% B solution for 3 min.

The samples were separated by HPLC and analyzed using a Q-Exactive mass spectrometer (Thermo Finnigan, San Jose, CA, USA) according to a previous method (Wang et al., 2016b). The analytical procedures were as follows: the time: 60 min; the detection method: positive ions; the scanning range of parent ions: 300–1800 m/z; the resolution of the high-quality MS1 spectra: 70,000 at m/z 200; AGC target: 3e6; the number of scan ranges: 1; and the dynamic exclusion: 40.0 s. The m/z ratios of polypeptide and polypeptide fragments were collected according to the following methods: 10 fragment maps (MS2 scanning) were collected after every full scanning, MS2 activation type: HCD, isolation window: 2 m/z, the resolution of the high-quality MS2 spectra: 17,500 at m/z 200, microscans: 1, normalized collision energy: 30 eV, underfill ratio: 0.1%.

#### 2.4. Identification and quantitative analysis of proteins

Mascot 2.2 software (Matrix Science, London, United Kingdom) and Proteome Discoverer 1.4 software (Thermo Fisher Scientific) was used for protein qualitative and quantitative analyses against the *K. candell* transcriptome database (Candel.Unigene.pep.fa, 45215 sequences) (Sandberg et al., 2012). In detail, the raw mass spectrometry data were searched with Mascot 2.2 software against the *K. candell* transcriptome database. The search parameters were: type of search: MS/MS Ion search; enzyme: trypsin; mass values: monoisotopic; max missed cleavages: 2; variable modifications: oxidation (Met) and iTRAQ-8plex (Tyr); peptide mass tolerance: ± 20 ppm; fragment mass tolerance: 0.1 Da. The data were screened according to the standard of FDR < 0.01, and high reliability protein qualitative results were obtained. The quantitation of the proteins was performed using Proteome Discoverer 1.4 software. The protein ratios were calculated as the median of only unique peptides of the protein. All the peptide ratios were normalized by the median protein ratio, and the median protein ratio should be 1 after the normalization. The proteins with fold change ratio of >1.2 or <0.83 and P-value of <0.05 were defined as differentially abundant proteins (DAPs).

#### 2.5. Functional classification of the DAPs

Based on three ontologies (cell component, biological process and molecular function), Gene Ontology (GO) function annotation (<http://www.geneontology.org>) was performed to map the sequences of DAPs. The Kyoto Encyclopedia of Genes and Genomes (KEGG) database (<http://www.genome.jp/kegg/> or <http://www.kegg.jp/>) was used for the KEGG pathway analysis of the DAPs.

#### 2.6. Western blot detection of heat shock proteins 70 (HSP70)

Western blot analysis was used to examine the abundance of HSP 70 using the method described by Wang et al. (2014). The sample proteins were separated using 12% SDS-PAGE electrophoresis, and a total of 50 μL of samples were loaded in each well. The proteins in the PAGE were transferred to a nitric acid fiber membrane using the semidry transfer method. Nitric acid fiber membrane was incubated in 0.2 mL cm<sup>-2</sup> blocking solution (5% skim milk powder dissolved in TBS buffer (10 mmol L<sup>-1</sup> Tris-HCl, 150 mmol L<sup>-1</sup> NaCl, pH 7.5) at room temperature and shaken slowly for 1 h. The nitric acid fiber membrane was washed using TBST buffer (0.05% Tween-20, 10 mmol L<sup>-1</sup> Tris-HCl, and 150 mmol L<sup>-1</sup> NaCl, pH 7.5). The membrane was further incubated in blocking solution with an HSP 70 antibody (1:5000, Agrisera, Vänås, Sweden) at room temperature for 1 h. The membrane was washed 3 times with TBST buffer for 5 min each, and it was incubated in alkaline phosphatase-crossed sheep antirabbit antibody (1:10,000, Huamei Bioengineering Company, Shanghai, China) overnight at 4 °C. Afterwards, the membrane was equilibrated in a new buffer (100 mmol L<sup>-1</sup> Tris-HCl, pH 9.5, 100 mmol L<sup>-1</sup> MgCl<sub>2</sub>) and transferred to chromogenic reagent, and the reaction was conducted as described by the manufacturer of the DAB Chromogenic Kit (AR1021, Boster Biological Technology Co., Ltd, Wuhan, China). The intensities of immunoreactive bands were quantified using software Image J (Bethesda, MD, USA), and three independent experiments were performed.

#### 2.7. Measurement of physiological and biochemical parameters

The hydroxylamine oxidation (Wang, 1990), titanium tetrachloride (TiCl<sub>4</sub>) colorimetry (Patterson et al., 1984a) and thiobarbituric acid (TBA) methods (Schmedes and Hølmer 1989) were used to determine the superoxide anion (O<sub>2</sub><sup>-</sup>), hydrogen peroxide (H<sub>2</sub>O<sub>2</sub>) and malondialdehyde (MDA) contents, respectively. The activities of superoxide dismutase (SOD), peroxidase (POD), catalase (CAT), ascorbate peroxidase (APX), and glutathione reductase (GR) were determined using NBT photoreduction (Hyland et al., 1983), guaiacol (Yu et al., 2011) and Patterson methods (Patterson et al., 1984b), as described by Nakano and Asada (1981) and Halliwell and Foyer (1978), respectively. The glutathione (GSH) and AsA and total triterpene contents were determined according to Law et al. (1983), Guri (1983) and as described in reference (Basyuni et al., 2012), respectively.

The activities of 6-phosphofructokinase (PFK), isocitrate dehydrogenase (IDH), succinate dehydrogenase (SDH), and malate dehydrogenase (MDH) were determined as described by the manufacturer of the corresponding kits (Suzhou Keming Biotechnology Co., Ltd, Suzhou, China). The activities of pyruvate kinase (PK)

and pyruvate decarboxylase (PDC) were assayed using the instructions of the kits developed by Nanjing Institute of Bioengineering.

### 3. Results

#### 3.1. Changes in the protein abundance of *K. candel* roots in response to high-salinity stress

Using iTRAQ analysis, a total of 286031 secondary mass spectra were obtained in *K. candel* root, of which 50264 were matched with specific peptides. In total, 25,441 peptides were identified, including 22,119 unique peptides, and 5577 proteins were identified. According to the fold change ratio of protein expression, abundance of  $>1.2$  or  $<0.83$  and P-value  $< 0.05$ , 227 DAPs were screened. Among them, 110 DAPs were up-regulated and 117 DAPs were down-regulated.

The DAPs in the *K. candel* roots that were subjected to NaCl treatment involved three ontologies (cell component, biological processes, and molecular function) as shown in Figure 1. Metabolic processes, cellular processes, and stress responses accounted for a large proportion of the biological processes. Cells, organelles, and cell membranes accounted for a large proportion of the cell composition. Binding molecule function and catalytic activity accounted for a large proportion of the molecular function. Fisher's exact test was used for GO enrichment analysis of the DAPs. The results showed that the DAPs in the *K. candel* roots subjected to NaCl treatment were

significantly enriched in enzymatic activities, carbohydrate metabolism, cell periphery, extracellular area, cell wall, and other functional items (Supplementary Figure 1). These results indicated that salt stress in *K. candel* roots primarily affect biological processes, such as carbohydrate and energy metabolisms and cell structure. Fisher's exact test was also used for KEGG enrichment analysis and the results showed that the KEGG was primarily enriched in phenylpropane biosynthesis, aminoglycose and nucleotide glycometabolism as well as starch and sucrose metabolism (Supplementary Figure 2).

#### 3.2. Functional classifications of the DAPs in *K. candel* roots in response to high-salinity stress

Based on the GO and KEGG analyses, functional classifications of highly reliable DAPs were conducted (Figure 2). The results showed that there were 11 functional classifications of DAPs in *K. candel* roots under NaCl treatment, including carbohydrate and energy metabolisms (17.62%), membrane and transport (12.78%), stress and defense (11.01%), signal transduction (10.57%), protein degradation and synthesis (7.05%), cytoskeleton and cell wall (6.61%), secondary metabolism (6.17%), RNA processing and metabolism (3.08%), transcription (3.08%), amino acid metabolism (1.76%), and unclassified proteins (20.26%). As shown in Table, most of the protein abundances involved in carbohydrate and energy metabolisms, secondary metabolism, stress response and defense, and cell structure were significantly increased,

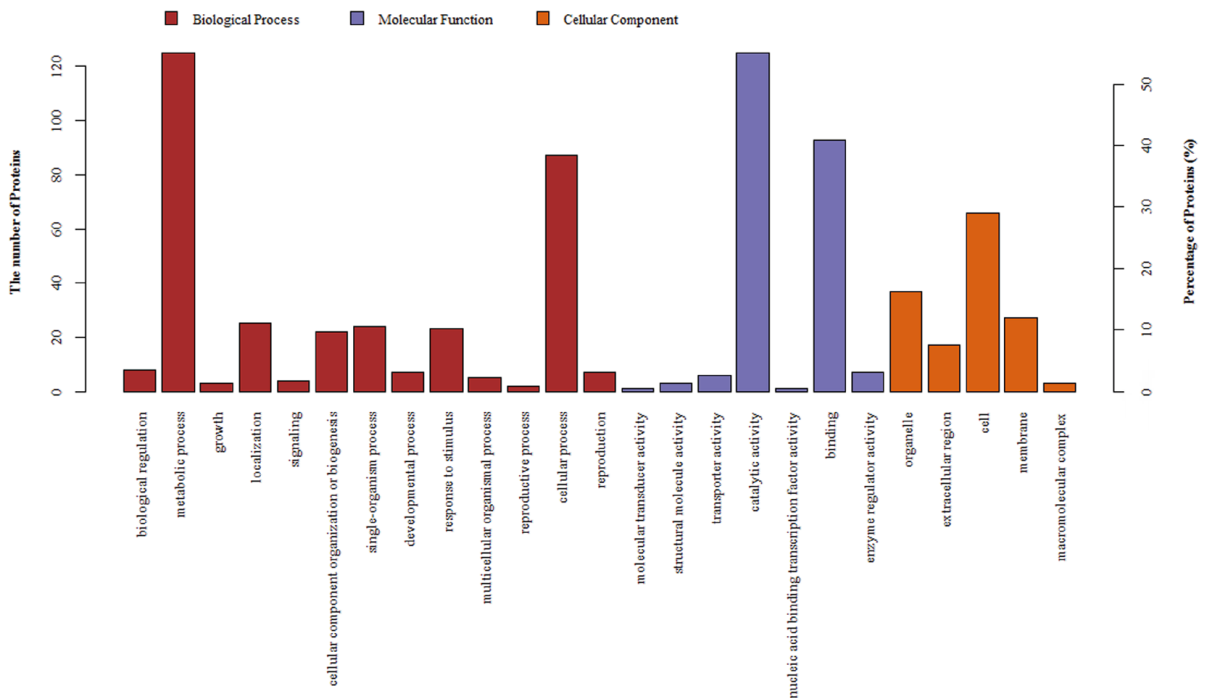


**Figure 1.** GO classification of differentially abundant proteins identified from *Kandelia candel* roots under high-salinity stress.

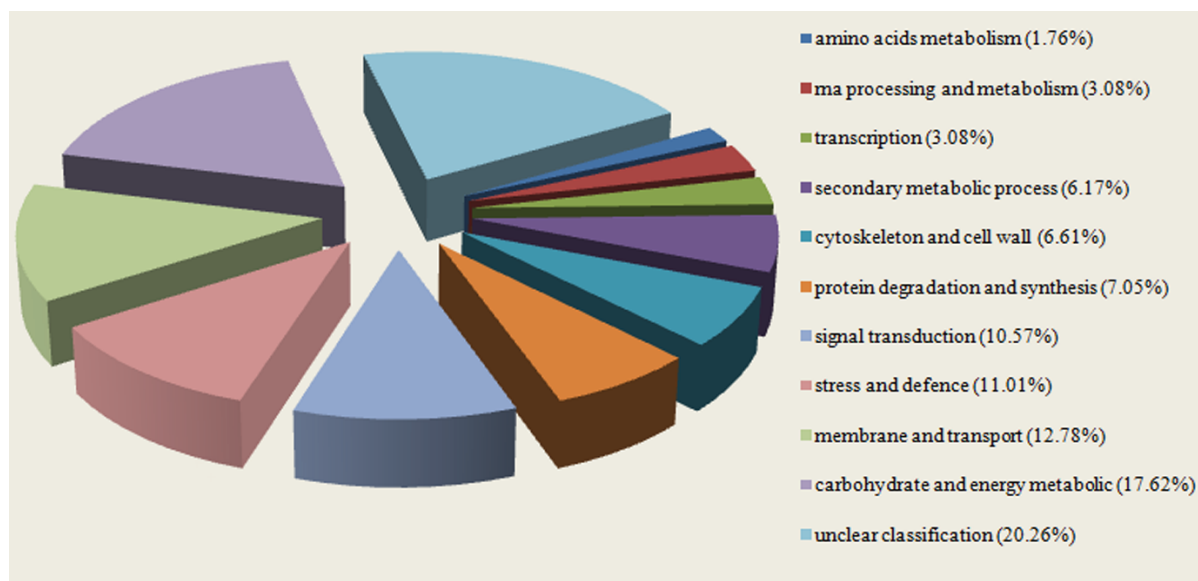


**Figure 2.** Functional classification of differentially abundant proteins identified from *Kandelia candel* roots under high-salinity stress.

indicating that the *K. candel* root responds actively to these metabolic pathways while under salt stress.

### 3.3. Western blot detection of HSP70

HSP 70 is an important stress responsive protein. In the present study, Western blot assay was used to verify the change in abundance of HSP70 in *K. candel* roots under high-salinity stress (Figure 3). The results showed that the protein abundance of HSP70 increased significantly under the 600 mmol L<sup>-1</sup> NaCl treatment, which was consistent with the iTRAQ results.

### 3.4. Physiological characteristics of *K. candel* roots in response to high-salinity stress

Under the 600 mmol L<sup>-1</sup> NaCl treatment, the O<sub>2</sub><sup>-</sup> and hydrogen H<sub>2</sub>O<sub>2</sub> content in the *K. candel* roots was significantly higher than that under the 0 mmol L<sup>-1</sup> NaCl treatment, while the MDA content increased slightly with no significant difference compared with that under the 0 mmol L<sup>-1</sup> NaCl treatment (Figure 4). The determination of the activities of antioxidant enzymes and the contents of antioxidant substances in *Kandelia candel* roots showed that the activities of SOD, POD, CAT, APX, and GR, and the contents of antioxidants (GSH and AsA) also increased significantly under 600 mmol L<sup>-1</sup> NaCl treatment as compared to 0 mmol L<sup>-1</sup> NaCl treatment (Figure 4). In addition, total triterpenes accumulated to a significant level in *K. candel* roots under high-salinity stress (Figure 4).

The Embden-Meyerhof-Parnas and tricarboxylic acid (EMP-TCA) pathway is the primary source of energy supply in plants. In this study, the key enzymes in the EMP-TCA pathway were determined and the results are

shown in Figure 5. Compared to the 0 mmol L<sup>-1</sup> NaCl treatment, the activities of PFK, PK, PDC, IDH, SDH, and MDH in the EMP-TCA pathway under 600 mmol L<sup>-1</sup> NaCl treatment increased significantly.

## 4. Discussion

### 4.1. Carbohydrate and energy metabolisms

It has been found that 9.9%, 21%, and 34.7% of the DAPs participate in carbohydrate and energy metabolisms in response to salt stress in *Raphanus sativus* roots and *Musa paradisiaca* and *A. marina* leaves, respectively (Sun et al., 2017; Shen et al., 2018b; Ji et al., 2019). Previous studies indicated that the effective regulation of protein expression in carbohydrate and energy metabolisms in *H. glomeratus* and *G. hirsutum* roots played important roles in their salt tolerance (Li et al., 2015; Wang et al., 2016a). The roots of the salt-tolerant maize inbred line Jing724 were found to improve in their salt tolerance by enhancing energy supply (Luo et al., 2017). Shen et al. (2018a) reported that salt-tolerant wild barley roots could maintain a normal supply of energy by up-regulating the expression of some key enzymes and proteins involved in the EMP-TCA pathway under salt stress to adapt to a high salt environment. These results suggest that carbohydrate and energy metabolisms play important roles in plant responses to salt stress. Herein, we found that 17.62% of DAPs in *K. candel* roots were involved in carbohydrate and energy metabolisms under high-salinity stress. In plants, the EMP-TCA pathway is the most important biological process in carbohydrate and energy metabolisms. It does not only meet the energy needs of the organism but also

**Table.** Some key differentially abundant proteins from iTRAQ result in *K. candel* roots under high-salinity stress.

| Accession                                 | Protein name                                       | Coverage/% | MW/kDa | pI   | UP | average 600 mM/0 mM | t-test P-value |
|---|--|------------|--------|------|----|---------------------|----------------|
| <b>Carbohydrate and energy metabolism</b> |  |            |        |      |    |                     |                |
| comp19949_c0                              | UDP-d-glucose 4-epimerase 1                        | 34.2       | 38.9   | 7.14 | 9  | 1.331               | 0.020          |
| comp15041_c0                              | 6-phosphofructokinase 3                            | 17.0       | 61.3   | 7.08 | 5  | 1.736               | 0.011          |
| CL13463Contig1                            | Fructokinase 2                                     | 25.9       | 41.4   | 6.37 | 5  | 1.297               | 0.014          |
| CL12703Contig1                            | Pyruvate kinase isozyme A                          | 19.0       | 63.5   | 5.91 | 8  | 1.303               | 0.010          |
| CL3374Contig1                             | Pyruvate decarboxylase 2                           | 22.0       | 65.1   | 6.28 | 9  | 1.799               | 0.011          |
| CL336Contig2                              | Pyruvate dehydrogenase kinase isoform 1            | 32.1       | 41.6   | 6.47 | 8  | 1.520               | 0.021          |
| CL8767.Contig2_All                        | Malate dehydrogenase, mitochondrial (Precursor)    | 59.9       | 36.0   | 8.18 | 7  | 1.219               | 0.012          |
| CL362Contig2                              | ATP-citrate synthase                               | 30.3       | 46.7   | 5.57 | 7  | 1.447               | 0.007          |
| CL4267.Contig4_All                        | Aconitate hydratase 2                              | 41.6       | 109.0  | 7.17 | 9  | 1.548               | 0.015          |
| Unigene3760_All                           | Phosphoglycerate kinase                            | 66.9       | 18.5   | 4.77 | 6  | 1.288               | 0.021          |
| CL10577Contig1                            | Isocitrate dehydrogenase                           | 51.0       | 46.9   | 7.97 | 9  | 1.204               | 0.010          |
| Unigene16086_All                          | Succinate dehydrogenase 5                          | 40.5       | 26.5   | 6.14 | 6  | 1.351               | 0.012          |
| CL8363.Contig1_All                        | Cytochrome c oxidase subunit 6b-1-like             | 15.5       | 21.5   | 4.35 | 3  | 1.204               | 0.037          |
| <b>Secondary metabolism</b>               |  |            |        |      |    |                     |                |
| comp22281_c0                              | 1-deoxy-d-xylulose-5-phosphate                     | 3.5        | 78.0   | 7.36 | 1  | 2.016               | 0.021          |
| CL8869Contig1                             | 2-c-methyl-d-erythritol -cyclodiphosphate synthase | 21.5       | 25.8   | 8.57 | 4  | 1.219               | 0.004          |
| comp21082_c0                              | Flavonoid o-methyltransferase related              | 8.0        | 40.1   | 6.58 | 2  | 1.286               | 0.001          |
| CL773.Contig6_All                         | 2-oxoglutarate fe -dependent dioxygenase-like      | 11.2       | 10.8   | 8.85 | 1  | 1.643               | 0.028          |
| CL5146Contig1                             | Trehalose-phosphate synthase                       | 10.4       | 96.6   | 6.35 | 4  | 1.232               | 0.002          |
| comp30356_c0                              | Anthocyanidin synthase                             | 7.3        | 10.9   | 7.37 | 1  | 0.732               | 0.049          |
| CL11481Contig1                            | Chalcone synthase                                  | 20.8       | 42.4   | 6.80 | 1  | 0.819               | 0.003          |
| comp7691_c0                               | S-adenosylmethionine-dependent methyltransferase   | 16.7       | 26.2   | 6.55 | 3  | 1.366               | 0.006          |
| CL10439Contig1                            | Myo-inositol oxygenase                             | 22.2       | 36.5   | 5.30 | 7  | 1.314               | 0.015          |
| CL7327.Contig2_All                        | Dihydroneopterin aldolase-like isoform 1           | 18.8       | 14.9   | 7.68 | 1  | 1.336               | 0.020          |
| comp5773_c0                               | Polyphenol oxidase                                 | 39.9       | 66.7   | 7.24 | 19 | 1.303               | 0.006          |
| comp20983_c0                              | Caffeic acid 3-o-methyltransferase                 | 15.8       | 40.2   | 5.71 | 4  | 0.781               | 0.008          |
| <b>Stress response and defense</b>        |  |            |        |      |    |                     |                |
| comp19686_c0                              | Cationic peroxidase 2                              | 43.7       | 36.7   | 8.63 | 12 | 1.695               | 0.004          |
| comp6524_c0                               | Peroxidase 52-like                                 | 46.1       | 33.9   | 9.58 | 11 | 1.436               | 0.041          |
| CL3111Contig1                             | Peroxidase superfamily protein                     | 52.1       | 36.2   | 9.72 | 12 | 1.894               | 0.002          |
| CL10686Contig1                            | Peroxidase superfamily protein                     | 27.1       | 34.8   | 9.35 | 6  | 1.292               | 0.010          |
| CL12322Contig1                            | Peroxidase 47-like                                 | 12.3       | 34.4   | 5.77 | 3  | 0.793               | 0.036          |
| CL91Contig2                               | Catalase family protein                            | 43.5       | 56.9   | 7.40 | 13 | 1.202               | 0.006          |
| Unigene1381_All                           | Tau class glutathione transferase gstu52           | 21.9       | 17.6   | 9.11 | 3  | 1.247               | 0.041          |
| comp6225_c0                               | Glutathione-disulfide reductase isoform 1          | 51.9       | 53.5   | 6.37 | 19 | 1.219               | 0.006          |
| comp6062_c0                               | OAS-tl3 cysteine synthase                          | 37.9       | 40.3   | 8.56 | 11 | 1.246               | 0.011          |
| CL6431.Contig1_All                        | Cysteine proteinase                                | 69.6       | 12.6   | 5.57 | 10 | 1.447               | 0.020          |
| Unigene17872_All                          | ATP sulfurylase                                    | 21.2       | 51.6   | 8.53 | 1  | 1.398               | 0.010          |
| Unigene4466_All                           | S-adenosylmethioninesynthetase                     | 58.3       | 43.0   | 6.05 | 1  | 0.710               | 0.007          |
| CL1465Contig1                             | heat shock protein                                 | 18.1       | 18.4   | 5.74 | 1  | 1.231               | 0.011          |

Table. Continued.

| Cell wall and others |   |      |      |      |   |       |       |
|----------------------|---|------|------|------|---|-------|-------|
| comp5806_c0          | Pectinesterase inhibitor 6-like                       | 14.7 | 58.1 | 7.69 | 6 | 1.432 | 0.010 |
| CL5352.Contig2_All   | Pectate lyase 15-like                                 | 5.7  | 27.2 | 5.99 | 1 | 0.821 | 0.022 |
| comp10840_c0         | Pectin methylesterase family protein                  | 18.0 | 57.2 | 9.41 | 8 | 0.685 | 0.035 |
| Unigene2986_All      | Xyloglucan endo-transglucosylase hydrolase protein 22 | 17.4 | 32.2 | 7.77 | 4 | 0.793 | 0.021 |
| CL11183Contig1       | Endochitinase pr4                                     | 38.2 | 28.6 | 7.64 | 9 | 1.792 | 0.021 |

Accession: Database accession numbers according to transcriptome.

Coverage: Percent sequence coverage of identified proteins.

MW: Theoretical mass (kDa) of identified proteins.

*pl*: *pI* of identified proteins.

UP: Number of unique peptides identified for each protein.

average 600 mM/0 mM: average protein abundance of 600 mmol L<sup>-1</sup> NaCl group vs. 0 mmol L<sup>-1</sup> NaCl group.

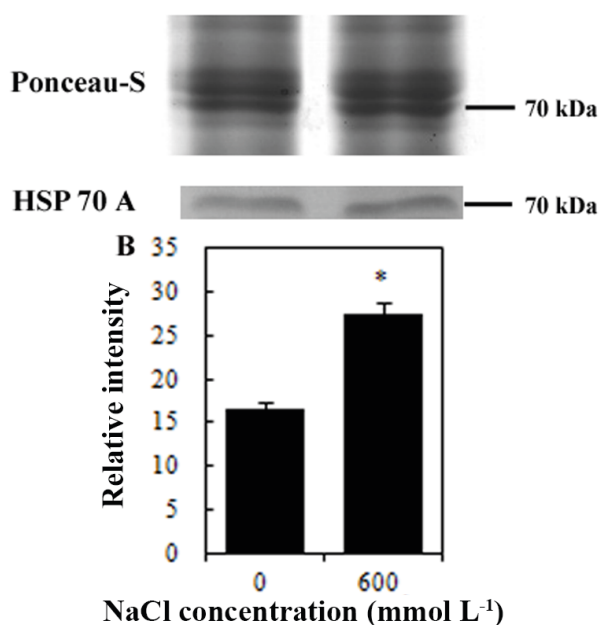


**Figure 3.** Western blot analysis of HSP 70 in *Kandelia candel* roots under high-salinity stress. Ponceau-S staining was used as loading control. (A) the result of western blot; (B) relative intensity of HSP 70. “\*” above the bar indicates a significant difference versus the 0 mmol L<sup>-1</sup> NaCl group at  $P < 0.05$ .

provide a variety of intermediates for other metabolic processes (Plaxton and Podestá 2006). The EMP process oxidizes glucose to pyruvate and produces ATP. In this process, PFK, phosphoglycerate kinase (PGK), and PK are the key rate-limiting enzymes. In this study, *K. candel* significantly increased the protein abundances of 6-PFK3 (comp15041\_c0), pyruvate kinase isomerase A

(CL12703 Contig1), and PGK (Unigene 3760\_All) under high-salinity stress (Table 1). The TCA cycle completely oxidizes the pyruvate produced by glycolysis into CO<sub>2</sub> and generates a large amount of ATP to sustain life (Sweetlove et al. 2010). Citrate synthase (CS), IDH and  $\alpha$ -ketoglutarate dehydrogenase are important rate-limiting enzymes in the TCA cycle. Under high-salinity stress, the abundances of pyruvate dehydrogenase kinase (PDK) isomer 1, pyruvate decarboxylase 2 (PDC2), ATP-CS, MDH, IDH, SDH and cytochrome oxidase C (Cyt c) subunits in *K. candel* roots increased significantly. The activities of EMP-related enzymes, including PFK, PK, PDC, and the TCA cycle-related enzymes, including PDC, IDH, MDH, and SDH, in *K. candel* roots increased significantly under high-salinity stress, which was consistent with our results of proteome analysis. Therefore, the up-regulation of these important proteins and enzyme activities in the EMP-TCA pathway in *K. candel* roots ensured the normal EMP-TCA pathway and provided sufficient energy for the plant to improve various metabolic processes under a high-salinity environment. Besides the up-regulation of EMP-TCA pathway, increased photosynthesis also plays a crucial role in improving salt tolerance in *K. candel* leaves under salt stress (Wang et al., 2014, 2015, 2016b).

#### 4.2. Stress response and defense

Salt stress leads to accumulation of ROS, which leads to the oxidative damage of lipids, proteins and nucleic acids, resulting in the disorder of normal metabolic processes (Parida et al., 2005). Plants can resist ROS-caused oxidative damage by producing various antioxidant enzymes and some other antioxidants (Gill et al., 2010). Previous studies demonstrated that SOD and POD proteins accumulate to high levels in tomato, cotton and wheat under salt stress (Guo et al. 2012; Gong et al. 2014; Li et al. 2015). The up-regulation of proteins related to stress responses and defense in *H. glomeratus* (Wang et al., 2016a) and

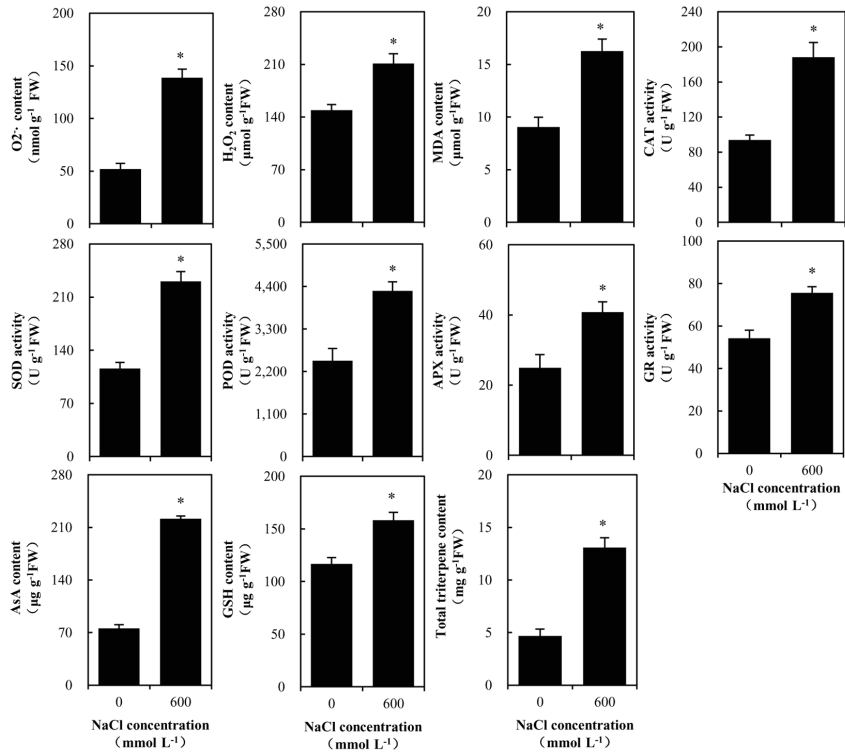


**Figure 4.** Changes in antioxidative ability and total triterpene content in *Kandelia candel* roots under high-salinity stress. Error bars indicate standard errors of three biological replicates. ‘\*’ above the bar indicates a significant difference versus the 0 mmol L<sup>-1</sup> NaCl group at P < 0.05.

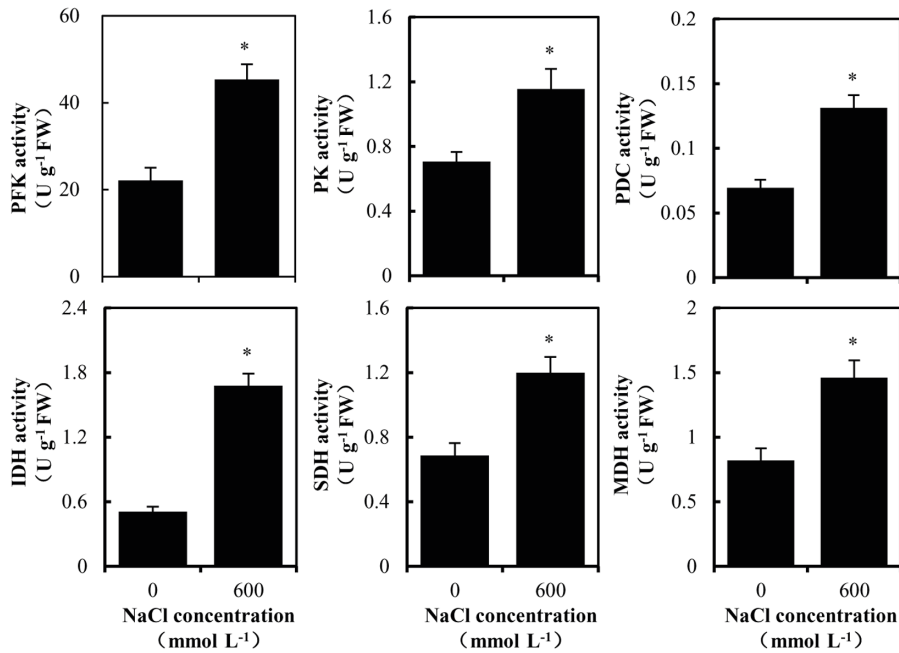


**Figure 5.** Analysis of EMP-TCA cycle in *Kandelia candel* roots under high-salinity stress. Error bars indicate standard errors of three biological replicates. ‘\*’ above the bar indicates a significant difference versus the 0 mmol L<sup>-1</sup> NaCl group at P < 0.05.

*G. max* cv Dongnong 50 (Ji et al., 2016) increases their salt tolerance. Furthermore, increased activities of some enzymes related to antioxidant contributed to enhancement of salt tolerance in wheat (*T. aestivum*) roots (Jiang et al., 2017). In this study, our results showed that the protein abundances of four PODs and one CAT in *K. candell* roots increased significantly under high-salinity stress, and the activities of SOD, POD, APX, and CAT also increased significantly. As antioxidants, AsA and GSH participate in the plant resistance to salt stress (Lü et al., 2016). GSH combines with peroxides and free radicals under the action of glutathione transferase (GST) to scavenge excessive ROS and protect the sulfhydryl group of proteins from being destroyed. In transgenic rice and tomato, the accumulation of GST helps the plants adapt to a salt stress environment (Takesawa et al., 2002; Xu et al., 2015b). Under salt stress, the abundance of GST protein in the mangrove *B. gymnorhiza* leaves increases significantly (Zhu et al. 2012). The present study also found that the contents of GST, GSH, and ASA, as well as GR activity increased significantly in *K. candell* roots in response to high-salinity stress. Although the ROS ( $O_2^-$  and  $H_2O_2$ ) content in the *K. candell* roots increased significantly under high-salinity stress, the MDA content did not increase significantly. Similar to the response to salt stress in *K. candell* leaves (Wang et al., 2014, 2015, 2016b), the roots might also initiate antioxidant systems to remove excess ROS and maintain balance of the redox state in the cells under high-salinity stress.

HSPs are stress-responsive proteins which play a crucial role in protecting plants against stress by refolding proteins (Zhu et al., 2012). The up-regulation of HSPs induced by salt stress has been observed in *Physcomitrella patens* (Wang et al., 2008), *Porteresia coarctata* (Sengupta and Majumder 2009), *B. gymnorhiza* (Zhu et al., 2012) and *Medicago sativa* (Xiong et al., 2017). In the present study, the abundance of HSP increased due to 600 mmol L<sup>-1</sup> NaCl treatment, indicating its protective function to the plant roots during high salinity.

#### 4.3. Cell wall structure and stability

The cell wall is a networked structure composed of polysaccharides, enzymes, and structural proteins, and it is the outermost barrier of plant cells (Micheli 2001). The cell wall first senses stress signals and transduces them into the cells to regulate cellular activities (Kong et al. 2010). Polysaccharides are the primary components of plant cell walls. Changes in the expression of proteins involved in the regulation of cell wall carbohydrates are essential for plants to respond to external stresses. This study found that the protein abundance of xyloglucan endo-transglucosylase hydrolase protein 22 (XTH22) in *K. candell* root was down-regulated, indicating that the *K. candell* root might reduce the decomposition reaction of polysaccharides in the cell wall to maintain the integrity and stability of the cell wall,

thereby improving its salt tolerance. Pectin is another major component of plant cell walls. Pectin methylesterase (PME) catalyzes the hydrolysis of pectin methoxy ester to pectic acid and methanol (Lionetti et al., 2007). Balestrieri et al., (1990) found that PME inhibitors form reversible noncovalent complexes with PME in kiwifruit, thus regulating the formation of pectin. We found herein that the expressions of pectin lyase and pectin methylesterase proteins were down-regulated in salt-stressed *K. candell* roots while the expression of a PME inhibitor was up-regulated under the same condition. This indicates that the *K. candell* root enhanced its cell wall stability through accumulation of pectin to resist high-salinity stress.

#### 4.4. Triterpenoids and cysteine metabolism

Terpenoids are secondary metabolites in plants and play important roles in plant growth and development, in addition to resistance to abiotic stress (de Costa et al., 2013). In this study, we found that salt stress induced the up-regulation of deoxyketose pentose phosphate (DXS) and 2-C-methyl-D-erythritol cyclophosphate synthase (MEP) proteins related to terpenoid metabolism in *K. candell* roots. Determination of total triterpenoids in the *K. candell* roots showed that the total content of these secondary metabolites increased under high-salinity stress which confirms our results of proteome analysis. Therefore, we postulated that the synthesis of terpenoids might be closely related to the response of *K. candell* roots to high-salinity stress.

Amino acids accumulate in plants under salt stress to protect intracellular nucleic acids, proteins, lipids, and other biomacromolecules from ROS attacks. Moreover, amino acids can also be used as compatible substances to participate in cell osmotic regulation and maintain intracellular pH stability. In this study, we found that the abundances of three cysteine synthesis-related proteins, including cysteine synthase, ATP sulfurylase, and cysteine proteinase, were up-regulated in *K. candell* roots under high-salinity stress. At the same time, cysteine can be desulfurized by the action of L-cysteine desulfhydrase and D-cysteine desulfhydrase, releasing H<sub>2</sub>S (Calderwood and Kopriva, 2014). As a plant signaling molecule, H<sub>2</sub>S is involved in multiple biological processes, such as alleviating the damage caused by abiotic stresses such as drought, osmosis, and metal ions (Jin et al., 2011). Therefore, we hypothesize that the up-regulation of cysteine synthesis-related protein in *K. candell* roots might be related to the initiation of H<sub>2</sub>S signaling pathway in response to high-salinity stress. Furthermore, phenylpropanoids and some free amino acids like  $\gamma$ -aminobutyric acid and glutamate were shown to play an important role in salt tolerance in *K. candell* leaves (Wang et al. 2016b).

In this study, our proteomic and physiological profiles provided important information of salt tolerant regulation network in the woody halophyte *K. candell* roots under

600 mmol L<sup>-1</sup> NaCl stress for 3 days. We found that carbohydrate and energy metabolisms, stress response and defense, cell wall structure, and secondary metabolites were involved in salt tolerance in *K. candel* roots. Together with the similar physiological profile changes, these findings indicate that *K. candel* roots under high-salinity stress could maintain cell energy supply through up-regulation of the EMP-TCA pathway, regulation of ROS balance by enhancing antioxidation-related enzyme activities and antioxidant contents, stabilizing cell wall structure by reducing polysaccharide decomposition and accumulating pectin, and adjusting cell osmosis through accumulation of triterpenes and other substances. The

study expands our knowledge on high-salt adaptation in woody plants and contributes to designing and developing salt-tolerant plants in the future.

### Acknowledgments

This work was supported by the Chinese National Natural Science Funds (Grant no. 331070542), the Natural Science Foundation of Fujian Province, China (Grant no. 2019J01819), Forestry Scientific Research Projects in Public Interest of China (Grant no. 201504415), and the Higher School of Applied Discipline Construction Project of Fujian Province, China (No. 44 document in 2017).

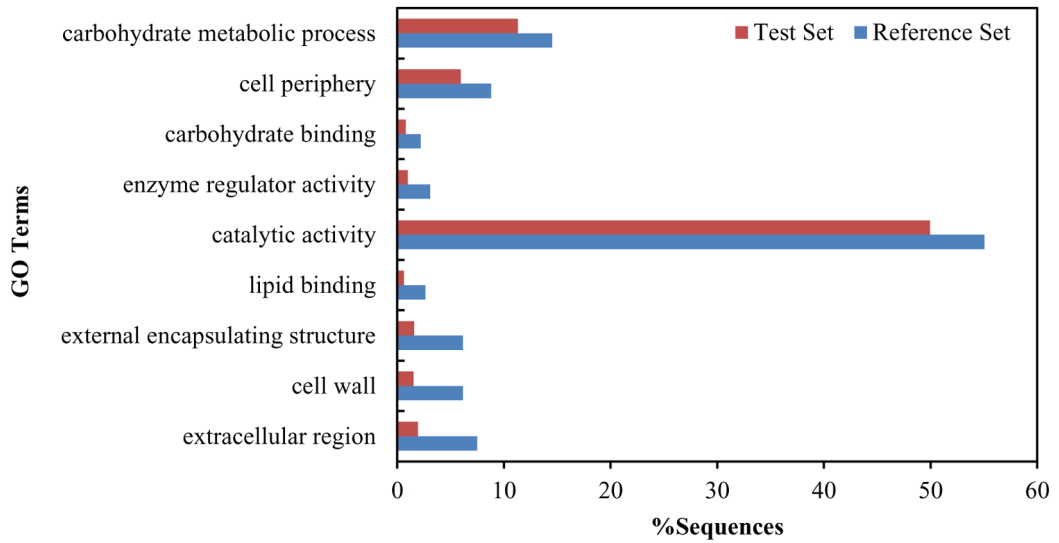
### References

- Balestrieri C, Castaldo D, Giovane A, Quagliuolo L, Servillo L (1990). A glycoprotein inhibitor of pectin methylesterase in kiwi fruit (*Actinidia chinensis*). *European Journal of Biochemistry* 193: 183-187. doi: 10.1271/bbb.60483
- Bandehagh A, Salekdeh GH, Toorchi M, Mohammadi A, Komatsu S (2011). Comparative proteomic analysis of canola leaves under salinity stress. *Proteomics* 11: 1965-1975. doi: 10.1002/pmic.201000564
- Basyuni M, Baba S, Kinjo Y, Putri LA, Hakim L et al. (2012). Salt-dependent increase in triterpenoids is reversible upon transfer to fresh water in mangrove plants *Kandelia candel* and *Bruguiera gymnorrhiza*. *Journal of Plant Physiology* 169: 1903-1908. doi: 10.1016/j.jplph.2012.08.005
- Bradford MM (1976). A rapid and sensitive method for the quantitation of microgram quantities of protein utilizing the principle of protein-dye binding. *Analytical Biochemistry* 72: 248-254. doi: 10.1016/0003-2697(76)90527-3
- Calderwood A, Kopriva S (2014). Hydrogen sulfide in plants: from dissipation of excess sulfur to signaling molecule. *Nitric Oxide* 41: 72-78. doi: 10.1016/j.niox.2014.02.005
- Cheng X, Deng G, Su Y, Liu JJ, Yang Y et al. (2016). Protein mechanisms in response to NaCl-stress of salt-tolerant and salt-sensitive industrial hemp based on iTRAQ technology. *Industrial Crops Prod* 83: 444-452. doi: 10.1016/j.indcrop.2015.12.086
- de Costa F, Yendo ACA, Fleck JD, Gosmann G, Fett-Neto AG (2013). Accumulation of a bioactive triterpene saponin fraction of *Quillaja brasiliensis* leaves is associated with abiotic and biotic stresses. *Plant Physiology and Biochemistry* 66: 56-62. doi: 10.1016/j.plaphy.2013.02.003
- Gill SS, Tuteja N (2010). Reactive oxygen species and antioxidant machinery in abiotic stress tolerance in crop plants. *Plant Physiology and Biochemistry* 48: 909-930. doi: 10.1016/j.plaphy.2010.08.016
- Gong B, Zhang C, Li X, Wen D, Wang S et al. (2014). Identification of NaCl and NaHCO<sub>3</sub> stress responsive proteins in tomato roots using iTRAQ-based analysis. *Biochemical and Biophysical Research Communications* 446: 417-422. doi: 10.1016/j.bbrc.2014.03.005
- Gong W, Xu F, Sun J, Peng Z, He S et al. (2017). iTRAQ-based comparative proteomic analysis of seedling leaves of two upland cotton genotypes differing in salt tolerance. *Frontiers in Plant Science* 8: 2113. doi: 10.3389/fpls.2017.02113
- Guo G, Ge P, Ma C, Li X, Lv D et al. (2012). Comparative proteomic analysis of salt response proteins in seedling roots of two wheat varieties. *Journal of Proteomics* 75: 1867-1885. doi: 10.1016/j.jprot.2011.12.032
- Guri ASAF (1983). Variation in glutathione and ascorbic acid content among selected cultivars of *Phaseolus vulgaris* prior to and after exposure to ozone. *Canadian Journal of Plant Science* 63: 733-737. doi: 10.4141/cjps83-090
- Halliwell B, Foyer C (1978). Properties and physiological function of a glutathione reductase purified from spinach leaves by affinity chromatography. *Planta* 139: 9-17. doi: 10.2307/23373245
- Hyland K, Voisin E, Banoun H, Auclair C (1983). Superoxide dismutase assay using alkaline dimethylsulfoxide as superoxide anion-generating system. *Analytical Biochemistry* 135: 280-287. doi: 10.1016/0003-2697(83)90684-x
- Ji FS, Tang L, Li YY, Wang WC, Yang Z et al. (2019). Differential proteomic analysis reveals the mechanism of *Musa paradisiaca* responding to salt stress. *Molecular Biology Reports* 46: 1057-1068. doi: 10.1007/s11033-018-4564-2
- Ji W, Cong R, Li S, Li R, Qin Z et al. (2016). Comparative proteomic analysis of soybean leaves and roots by iTRAQ provides insights into response mechanisms to short-term salt stress. *Frontiers in Plant Science* 7: 573. doi: 10.3389/fpls.2016.00573

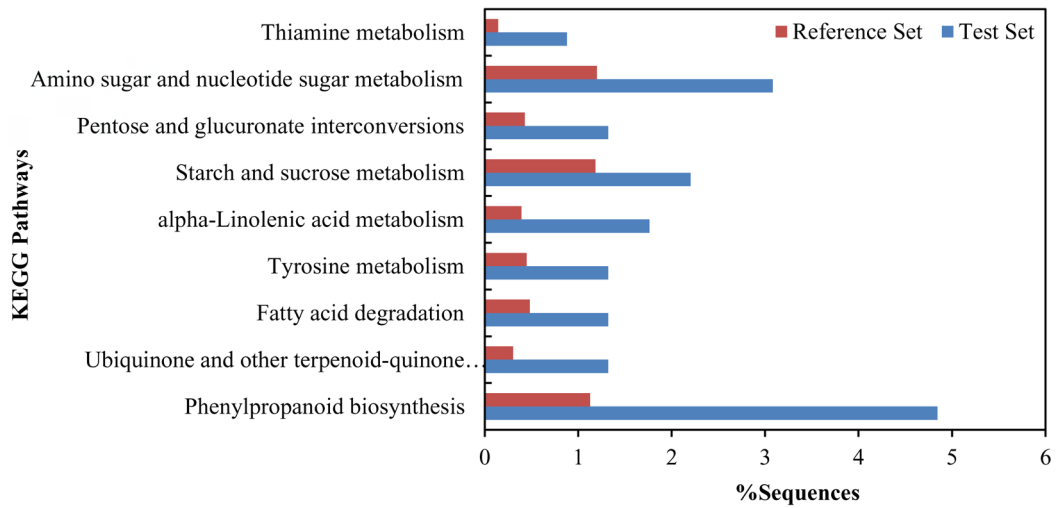
- Jiang Q, Li X, Niu F, Sun X, Hu Z et al. (2017). iTRAQ - based quantitative proteomic analysis of wheat roots in response to salt stress. *Proteomics* 17: 265. doi: 10.1002/pmic.201600265
- Jin Z, Shen J, Qiao Z, Yang G, Wang R et al. (2011). Hydrogen sulfide improves drought resistance in *Arabidopsis thaliana*. *Biochemical and Biophysical Research Communications*. 414: 481-486. doi: 10.1016/j.bbrc.2011.09.090
- Kong FJ, Oyanagi A, Komatsu S (2010). Cell wall proteome of wheat roots under flooding stress using gel-based and LC MS/MS-based proteomics approaches. *Biochimica et Biophysica Acta -Proteins and Proteomics* 1804: 124-136. doi: 0.1016/j.bbapap.2009.09.023
- Kosová K, Vítámvás P, Prášil IT, Renaut J (2011). Plant proteome changes under abiotic stress-contribution of proteomics studies to understanding plant stress response. *Journal of Proteomics* 74: 1301-1322. doi: 10.1016/j.jprot.2011.02.006
- Law M, Charles SA, Halliwell B (1983). Glutathione and ascorbic acid in spinach (*Spinacia oleracea*) chloroplasts. The effect of hydrogen peroxide and of paraquat. *Biochemical Journal* 210: 899-903. doi: 10.1042/bj2100899
- Li W, Zhao FA, Fang W, Xie D, Hou J et al. (2015). Identification of early salt stress responsive proteins in seedling roots of upland cotton (*Gossypium hirsutum* L.) employing iTRAQ-based proteomic technique. *Frontiers in Plant Science* 6: 732. doi: 10.3389/fpls.2015.00732
- Lionetti V, Raiola A, Camardella L, Giovane A, Obel N et al. (2007). Overexpression of pectin methylesterase inhibitors in *Arabidopsis* restricts fungal infection by *Botrytis cinerea*. *Plant Physiology* 143: 1871-1880. doi: 10.2307/40065398
- Luo M, Zhao Y, Wang Y, Shi Z, Zhang P et al. (2017). Comparative proteomics of contrasting maize genotypes provides insights into salt-stress tolerance mechanisms. *Journal of Proteome Research* 17: 141-153. doi: 10.1021/acs.jproteome.7b00455
- Lü XM, Yang YF, Lu XY, Jin J, Fan XM (2016). Effects of NaCl stress on the AsA-GSH cycle in sour jujube seedlings. *Plant Physiology Journal* 52: 736-744 (in Chinese with an abstract in English). doi: 10.13592/j.cnki.ppj.2015.0706
- Micheli F (2001). Pectin methylesterases: cell wall enzymes with important roles in plant physiology. *Trends in Plant Science* 6: 414-419. doi: 10.1016/S1360-1385(01)02045-3
- Miyazaki Y, Hiraide M, Shibuya H (2007). Molecular cloning of functional genes for high growth-temperature and salt tolerance of the basidiomycete *Fomitopsis pinicola* isolated in a mangrove forest in Micronesia. *Bioscience Biotechnology and Biochemistry* 71: 273-278. doi: 10.1271/bbb.60483
- Nakano Y, Asada K (1981). Hydrogen peroxide is scavenged by ascorbate-specific peroxidase in spinach chloroplasts. *Plant Cell Physiology* 22: 867-880. doi: 10.1093/oxfordjournals.pcp.a076232
- Pang Q, Chen S, Dai S, Chen Y, Wang Y (2010). Comparative proteomics of salt tolerance in *Arabidopsis thaliana* and *Thellungiella halophila*. *Journal of Proteome Research* 9: 2584-2599. doi: 10.1021/pr100034f
- Parida AK, Das AB (2005). Salt tolerance and salinity effects on plants: a review. *Ecotoxicology and Environmental Safety* 60: 324-349. doi: 10.1016/j.ecoenv.2004.06.010
- Patterson BD, MacRae EA, Ferguson IB (1984a). Estimation of hydrogen peroxide in plant extracts using titanium (IV). *Analytical Biochemistry* 139: 487-492. doi: 10.1016/0003-2697(84)90039-3
- Patterson BD, Payne LA, Chen YZ, Graham D (1984b). An inhibitor of catalase induced by cold in chilling-sensitive plants. *Plant Physiology* 76: 1014-1018. doi: 10.2307/4269048
- Plaxton WC, Podestá FE (2006). The functional organization and control of plant respiration. *Critical Reviews in Plant Sciences*. 25: 159-198. doi: 10.1080/07352680600563876
- Sandberg A, Lindell G, Källström BN, Branca RM, Danielsson KG et al. (2012). Tumor proteomics by multivariate analysis on individual pathway data for characterization of vulvar cancer phenotypes. *Molecular Cellular Proteomics* 11: M112. 016998. doi: 10.1074/mcp.M112.016998
- Schmedes A, Hölmer G (1989). A new thiobarbituric acid (TBA) method for determining free malondialdehyde (MDA) and hydroperoxides selectively as a measure of lipid peroxidation. *Journal of the American Oil Chemists Society* 66: 813-817. doi: 10.1007/bf02653674
- Sengupta S, Majumder AL (2009). Insight into the salt tolerance factors of a wild halophytic rice, *Porteresia coarctata*: a physiological and proteomic approach. *Planta*. 229: 911-929. doi: 10.1007/s00425-008-0878-y
- Shen Q, Yu J, Fu L, Wu L, Dai F et al. (2018a). Ionic, metabolomic and proteomic analyses reveal molecular mechanisms of root adaption to salt stress in Tibetan wild barley. *Plant Physiology Biochemistry* 123: 319-330. doi: 10.1016/j.plaphy.2017.12.032
- Shen Z, Chen J, Ghoto K, Hu W, Gao G et al. (2018b). Proteomic analysis on mangrove plant *Avicennia marina* leaves reveals nitric oxide enhances the salt tolerance by up-regulating photosynthetic and energy metabolic protein expression. *Tree Physiology* 38: 1605-1622. doi: 10.1093/treephys/tpy058
- Song Y, Zhang C, Ge W, Zhang Y, Burlingame, AL et al. (2011). Identification of NaCl stress-responsive apoplastic proteins in rice shoot stems by 2D-DIGE. *Journal of Proteomics* 74: 1045-1067. doi: 10.1016/j.jprot.2011.03.009
- Soni P, Nutan KK, Soda N, Nongpiur RC, Roy S et al. (2015). Towards understanding abiotic stress signaling in plants: Convergence of genomic, transcriptomic, proteomic, and metabolomic approaches. In: Pandey GK (editor). *Elucidation of Abiotic Stress Signaling in Plants*. New York, NY, USA: Springer, pp. 3-40. doi: 10.1007/978-1-4939-2211-6
- Sun X, Wang Y, Xu L, Li C, Zhang W et al. (2017). Unraveling the root proteome changes and its relationship to molecular mechanism underlying salt stress response in radish (*Raphanus sativus* L.). *Frontiers in Plant Science* 8: 1192. doi: 10.3389/fpls.2017.01192

- Sweetlove LJ, Beard KF, Nunes-Nesi A, Fernie AR, Ratcliffe RG (2010). Not just a circle: flux modes in the plant TCA cycle. *Trends in Plant Science* 15: 462-470. doi: 10.1016/j.tplants.2010.05.006
- Takesawa T, Ito M, Kanzaki H, Kameya N, Nakamura I (2002). Over-expression of  $\gamma$ -glutathione S-transferase in transgenic rice enhances germination and growth at low temperature. *Molecular Breeding* 9: 93-101. doi: 10.1023/A:1026718308155
- Tuteja N (2007). Mechanisms of high salinity tolerance in plants. In: Dieter H, Helmut S (editors). *Methods in Enzymology*. San Diego, CA, USA: Elsevier, pp. 419-438. doi: 10.1016/S0076-6879(07)28024-3
- Unwin RD, Griffiths JR, Whetton AD (2010). Simultaneous analysis of relative protein expression levels across multiple samples using iTRAQ isobaric tags with 2D nano LC-MS/MS. *Nature Protocols* 5: 1574. doi: 10.1038/nprot.2010.123
- Wang AG (1990). Quantitative relation between the reaction of hydroxylamine and superoxi-de anion radicals in plants. *Plant Physiology Communications* 26: 55-57. doi: 10.1021/ja00874a010
- Wang J, Yao L, Li B, Meng Y, Ma X et al. (2016a). Comparative proteomic analysis of cultured suspension cells of the halophyte *Halogeton glomeratus* by iTRAQ provides insights into response mechanisms to salt stress. *Frontiers in Plant Science* 7: 110. doi: 10.3389/fpls.2016.00110
- Wang L, Liu X, Liang M, Tan F, Liang W et al. (2014). Proteomic analysis of salt-responsive proteins in the leaves of mangrove *Kandelia candel* during short-term stress. *PLoS One* 9: e83141. doi: 10.1371/journal.pone.0083141
- Wang L, Pan D, Li J, Tan F, Hoffmann-Benning S et al. (2015). Proteomic analysis of changes in the *Kandelia candel* chloroplast proteins reveals pathways associated with salt tolerance. *Plant Science* 231: 159-172. doi: 10.1016/j.plantsci.2014.11.013
- Wang L, Pan D, Lv X, Cheng CL, Li J et al. (2016b). A multilevel investigation to discover why *Kandelia candel* thrives in high salinity. *Plant Cell Environment*. 39: 2486-2497. doi: 10.1111/pce.12804
- Wang XQ, Yang PF, Gao Q, Liu XL, Kuang TY et al. (2008). Proteomic analysis of the response to high-salinity stress in *Physcomitrella patens*. *Planta* 228:167-177. doi: 10.2307/23389955
- Xiong J, Sun Y, Yang Q, Tian H, Zhang H et al. (2017). Proteomic analysis of early salt stress responsive proteins in alfalfa roots and shoots. *Proteome Science* 15: 19. doi: 10.1186/s12953-017-0127-z
- Xu J, Lan H, Fang H, Huang X, Zhang H et al. (2015a). Quantitative proteomic analysis of the rice (*Oryza sativa* L.) salt response. *PLoS One* 10: e0120978. doi: 10.1371/journal.pone.0120978
- Xu J, Xing XJ, Tian YS, Peng RH, Xue Y et al. (2015b). Transgenic Arabidopsis plants expressing tomato glutathione S-transferase showed enhanced resistance to salt and drought stress. *PLoS One* 10: e0136960. doi: 10.1371/journal.pone.0136960
- Yu J, Chen S, Zhao Q, Wang T, Yang C et al. (2011). Physiological and proteomic analysis of salinity tolerance in *Puccinellia tenuiflora*. *Journal of Proteome Research* 10: 3852-3870. doi: 10.1021/pr101102p
- Zhu Z, Chen J, Zheng, HL (2012). Physiological and proteomic characterization of salt tolerance in a mangrove plant, *Bruguiera gymnorrhiza* (L.) Lam. *Tree Physiology* 32: 1378-1388. doi: 10.1093/treephys/tps097

Supplementary Figures



Supplementary Figure 1.



Supplementary Figure 2.